Accepted Manuscript

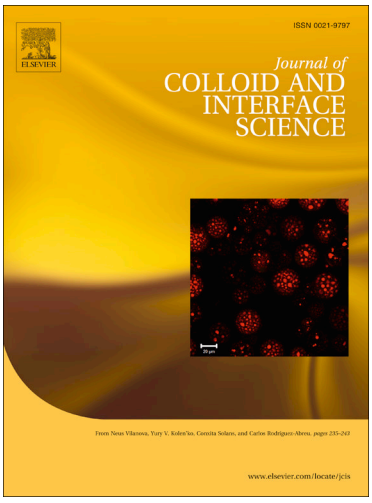

Self-propulsion of Aluminum Particle-Coated Janus Droplet in Alkaline Solution

Mengqi Li, Dongqing Li

PII: S0021-9797(18)30949-4
DOI: https://doi.org/10.1016/j.jcis.2018.08.034
Reference: YJCIS 23967

To appear in: *Journal of Colloid and Interface Science*

Received Date: 9 July 2018
Revised Date: 8 August 2018
Accepted Date: 10 August 2018

Please cite this article as: M. Li, D. Li, Self-propulsion of Aluminum Particle-Coated Janus Droplet in Alkaline Solution, *Journal of Colloid and Interface Science* (2018), doi: https://doi.org/10.1016/j.jcis.2018.08.034

Self-propulsion of Aluminum Particle-Coated Janus Droplet in Alkaline Solution

Mengqi Li and Dongqing Li*

Department of Mechanical and Mechatronics Engineering, University of Waterloo, Waterloo, Ontario, Canada N2L 3G1

*Corresponding author, Address: 200 University Ave. West, Waterloo, Ontario, N2L 3G1
Email: dongqing@uwaterloo.ca (D. Li)

Electronic supplementary information (ESI) is available.

Abstract

Janus droplet motion powered by gas bubbles is studied in this paper. The Janus droplets were fabricated by partially covering one side of an oil droplet with aluminum particles under gravity effect. By placing the Janus droplet in an alkaline solution, the reaction between the Al particles and OH^- generates H_2 gas, which emits from the particle-coated side of the droplet as bubbles. Hence, the droplet is propelled to move in the opposite direction. In this research, the effects of several factors, time, pH, particle coverage and surfactant, on the motion of the Janus droplet were studied. The experimental results indicate that as time progresses, the droplet motion experiences three periods: initial development stage, stable stage and decline stage. The speed of the droplet increases with the pH value and the particle coverage. Comparing with the other three surfactants, Tween 20, CTAB and SDS, the surfactant Triton X-100 is the best choice for generating the spontaneous motion of the Janus droplets. Furthermore, the directional motion of the Janus droplets was examined, and the results show that the controllable transportation of the Janus droplets can be accomplished by externally applied DC electric field. The spontaneous motion of the droplets offers great promise in chemical and biological applications.

Keywords: Self-propelled micromotor; Targeted transportation; aluminum particle; Janus droplet; Electric field.

1. Introduction

Manipulation of liquid droplets plays an important role in various applications, such as, mixing and separation, controllable drug delivery and food products dispersion[1–3]. However, the existing manipulation techniques rely on complex systems, including passive elements (channels) and external actuation systems (valves and pumps)[4–6]. The self-propelled motion of droplets provides a promising alternative pathway for manipulating droplets. The self-propulsion mechanisms of the droplets can be divided into the following categories: chemical reaction[7,8], solubilization[9,10], phase separation[11–13] and external stimuli[14–21]. For the mechanism of chemical reaction, the spontaneous motion of droplets results from the chemical reaction involving surfactants. Due to the reaction of the surfactant molecules on the oil-water interface, the interfacial tension along the surface of droplets becomes inhomogeneous, which leads to Marangoni flow at the interface and eventually drives the droplets to move in the continuous phase. For example, Toyota et al.[7] studied the self-propulsion of 4-octylaniline droplets containing catalyst in an aqueous surfactant solution. Reacting with the catalyst from the inside of the droplet, the surfactant molecules at the interface were hydrolyzed, breaking the interfacial symmetry and generating the spontaneous motion of the droplets. As the surfactant molecules from the bulk aqueous solution transfer to the interface continuously, the droplets keep moving by the reaction with the consumption of the surfactant molecules at the interface.

The solubilization mechanism of the self-propelled motion of droplets involves dissolving the droplets into surfactant micelles in the continuous phase. For a droplet immersed in a surfactant solution with the concentration significantly higher than the critical micelle concentration (CMC), some molecules of the droplet dissolve into the surfactant micelles and the size of the droplet decreases. As some surfactant molecules on the droplet are transferred together with the droplet molecules, a surfactant depletion region in vicinity of the droplet may occur. Generally, the solubilization process takes place non-uniformly, the surfactant along the surface of the droplet is distributed heterogeneously. Consequently, the Marangoni flow forms on the droplet, which in turn actuates the motion of the droplet. In 2011, Pimienta et al.[10] experimentally studied the spontaneous motion of water-saturated dichloromethane droplet in a cetyltrimethylammonium bromide (CTAB) solution. After dropping the droplet onto the surface of the aqueous phase, the droplet moves due to the solubilization of the droplet molecules. By studying the effect of CTAB

concentration on droplet motion systematically, they found that the spontaneous motion of the droplet can be generated only when the surfactant concentration of the aqueous phase is above the CMC value.

In addition, the droplets in a continuous phase can move spontaneously in a non-thermal equilibrium state. For an emulsion system, consisting of immiscible dispersed and continuous phases, when the system is in a far-from-thermal-equilibrium state, mass and momentum transfers on the droplet surfaces induce convection and spontaneous motion of the droplets. Self-propulsion of pure hexadecane droplet in acetone-rich phase was demonstrated by Molin's group[11]. Moreover, the motion of droplets can also be actuated by inducing interfacial tension gradient along suspended droplets with external stimuli, such as, heating[14], light illumination[15–17], electrical field[18,19] and chemical gradient field of the aqueous phase[20,21]. For example, Florea et al. [17] studied the spontaneous motion of a droplet under white light. In their system, a light-sensitive spiropyran sulfonic acid was dissolved into the aqueous phase. Under light irradiation, the H^+ ions are released and the local pH value of the aqueous phase decreases. With the generation of pH gradient in the aqueous phase between the light region and the dark region, the droplet moves away from the light source.

Recently, the development of Janus materials provides a new strategy in generating self-propelled micromotor. Janus materials possess asymmetrical structures with two sides carrying different physical or chemical properties. Therefore, under external stimuli or chemical reaction with the surrounding solution, the forces acting on the two sides of the Janus materials are unbalanced, which leads to the motion of the micromotors[22–24]. Based on the propulsion mechanism, the Janus micromotors can be divided into three major groups: self-electrophoresis[25,26], self-thermophoresis[27,28] and bubble propulsion. For self-electrophoresis, the two ends of the Janus micromotor are made from different conducting materials with different chemical potentials. After adding the motor into a buffer solution, due to the chemical reaction between the Janus micromotor and the buffer solution, a local current loop is generated between two ends of the micromotor; thus, the Janus micromotor is driven to move by electrophoresis. Self-thermophoresis generally uses a laser beam to induce a temperature gradient in the vicinity of the micromotor based on different absorptivity of its two sides, which in turn causes thermophoresis of the micromotor. Compared with these two mechanisms, the

bubble propulsion mechanism is most commonly used in actuating the motion of Janus micromotors. As the name suggests, the bubble propulsion motion results from the directional bubble ejection from the micromotor. By placing the Janus micromotor into chemical "fuel", one side of the micromotor starts a reaction and bubbles are ejected, i.e., via catalytic reaction or replacement reaction, to propel the micromotor towards the inactive side. The micromotor keeps moving until the chemical reactants are exhausted. For example, Gao et al.[29] showed the spontaneous motion of Al/Pd Janus microparticles in acid, alkaline and hydrogen peroxide solutions. In acid and alkaline solutions, hydrogen bubbles are generated in the Al side which drives the particle to move towards the Pd side; reversely, in hydrogen peroxide solution, catalytic reaction takes place on the Pd side to generate oxygen bubbles and the micromotor is propelled to move towards opposite direction.

However, most of the Janus micromotors reported in literatures are solid particles, which have the shortcomings of limited cargo loading capability and poor biodegradability. Therefore, research in developing new Janus droplet micromotors, combining the advantages of Janus materials and self-propelled droplets together, is highly desirable. Previously, we reported a novel Janus droplets fabrication method by partially covering the initially homogeneous oil micro-droplets with Al nano-particles under externally applied electrical field[30–35]. With the presence of the Al particle film, the Janus droplets can be utilized as bubble propulsion micromotors based on the chemical reaction of the Al particle with the surrounding acid or alkaline solution. In this paper, for the first time, the self-propulsion of the Janus droplets in alkaline solutions was demonstrated. The influence factors, including time, pH value of the surrounding solution, particle coverage of the Janus droplet and surfactant on the spontaneous motion of the Janus droplets were studied experimentally. Furthermore, the directionally controlled transportation of the Janus droplets was accomplished by using electrical field.

2. Materials and methods

2.1 Materials and chemicals

Non-ionic surfactants of Triton X-100 and Tween 20, cationic surfactant of CTAB and anionic surfactant of SDS, sodium hydroxide (NaOH) were purchased from Sigma-Aldrich. All the chemicals were of reagent grade and used without further treatment. Aluminum particles with an

average diameter of 10 μm were purchased from US Research Nanomaterials, Inc. Oil used in the analysis was canola oil (100% pure, Mazola Corporation). Deionized water (18.2 MΩ·cm) was obtained from Milli-Q purification system (Japan Millipore, Japan).

2.2 Preparation of Al particle-coated Janus droplets

The Janus droplets were prepared by dispersing oil containing Al particles into an aqueous solution, as shown in Figure S1 (see Supplementary Information). This method includes four steps. First, in order to prepare the particle-in-oil dispersion phase, 10 μm Al particles and 5 mL oil were added into a 15 mL-in-volume glass bottle. After vibrating the mixture with a lab dancer (VWR Scientific) at the maximum speed of 3200 rpm for 2 minutes, the particles are dispersed into oil uniformly. Then, 100 μL of the oil was dropped into the other glass bottle containing 5 mL Triton X-100 aqueous solution (2% (v/v)). The final position of the oily phase in the aqueous phase, floating at the top, suspending in the middle, or sinking at the bottom, is dependent on the amount of Al particles in it. After this, the three-phase mixture was shaken with the lab dancer at 3200 rpm for 30 seconds to form oil-in-water emulsion. Due to the vibration, the particles moved to the surface of emulsion droplets, and the Al particle film formed on the surface of each oil droplet. Because of the shield of the passivation oxide layer on the surfaces of the Al particles, the reaction between the aqueous phase and the Al particles is hampered. After vibration, the mixture was kept stationary for 10 min. Over this period of time, the Al particles were concentrated to the bottom of the droplets under gravity effect, and finally, the Janus droplets with the bottom side hemisphere covered with Al particles were formed.

The particle coverage of the Janus droplets generated with this method depends on the amount of particles on the surface of droplets. To generate Janus droplets with different particle coverages, particle-in-oil dispersions with different Al particle concentrations, ranging from 40 mg/mL to 280 mg/mL, were employed in fabricating the Janus droplets. The bright-field optical microscope (Nikon Ti-E, Nikon, Japan) was employed to examine the Janus droplets.

2.3 Analysis of the spontaneous motion of the Janus droplets

The experiments for the study of the spontaneous motions of the Janus droplets were carried out in the NaOH solutions. The experiments were conducted in a chamber with the size of 1 cm × 1 cm × 0.5 mm (Length × Width × Height), as shown in Figure S2 (a). The chamber was fabricated by bonding a PDMS layer containing chamber structure and a glass substrate (VWR Scientific)

together after plasma treatment (HARRICK PLASMA, Ithaca, NY, USA). In the experiments, after filling the reaction chamber with NaOH solution, the Janus droplets were added into the chamber with a digital pipette (Eppendorf Research). The spontaneous motions of the Janus droplets in alkali solutions were observed with an optical microscope (Nikon Ti-E), and the images were recorded by a CCD camera (DS-Qi1Mc, Nikon) at the speed of 25 fps. The recorded videos were analyzed with imaging analysis software. The motion velocities of the droplets were obtained by measuring the moving distance of the droplets over a time interval. For each experiment, 30 measurements were conducted to obtain the average velocity and the standard deviation. The Janus droplets with the diameter ranging from 70 μm to 100 μm were chosen to conduct analysis.

The effects of time, pH value of the aqueous solution, particle coverage and surfactant on the spontaneous motion of the Janus droplets were studied experimentally. In these studies, without special declaration, the alkaline solutions containing 2% (v/v) Triton X-100 were used. The Janus droplets generated from 280 mg/mL particle-in-oil dispersion and pH=14 aqueous solution were used in detecting the time effect. To test the self-propulsion motion of the Janus droplets in different pH solutions, the aqueous solutions containing different concentrations of NaOH were utilized. The velocity and life time of the Janus droplets generated from 280 mg/mL particle-in-oil dispersion in alkali solutions with pH ranging from 12 to 14 were measured. In the study of particle coverage effect, Janus droplets were generated from different concentrations of particle-in-oil dispersions, 40 mg/mL, 120mg/mL, 200 mg/mL and 280 mg/mL. The moving velocities of these Janus droplets in pH 14 solution were detected, respectively. Apart from Triton X-100, the other three surfactants, Tween 20, SDS and CTAB, were also introduced into the aqueous solution to study the surfactant effect. In the experiment, the moving status of the droplets in the alkali solutions with 2% (v/v) Tween 20, 1.2% (w/v) SDS and 1% (w/v) CTAB were observed under microscope, respectively.

2.4 Electrical navigation of the Janus droplets

To examine the electrical control of the motion of the Janus droplets, an experimental setup was built, which consists of a direct current (DC) power supplier, a voltage control unit, a reaction chamber and a Ti-E microscope, as shown in Figure S2(b). The electric field was supplied by the DC power supplier (CSI12001X, Circuit Specialist Inc., USA) with adjustable output voltage

ranging from 0V to 125V. The voltage control unit bridging between the power supplier and the reaction chamber was employed to control the direction of the electric field applied to the reaction chamber. The electric field was applied to the chamber through four electrodes inserted in the reservoirs. By placing the reaction chamber on the object stage of the microscope, the self-propulsion motion of the micromotors under the effect of electric field was observed by the microscope.

In the experiment, the reaction chamber was filled with aqueous alkali solution at pH 14 containing 2% (v/v) Triton X-100 first. After injecting the Janus droplet, the spontaneous motion of the droplet was triggered with bubble propulsion. By applying electric field of 25 V/cm to the reaction chamber, the droplet rotated to get aligned with the electric field because of the Al particle coating on one side of the droplet surface. Hence, the droplet moved along the electric field. Changing the direction of the electric field, the Janus droplet followed the orientation of the electric field, and the moving direction of it changed responsively. To avoid the electrolysis and Joule heating of the aqueous electrolyte, the electric field was applied intermittently. The maximum time for turning on the electric field each time is 2 second. The directional motion of Janus micromotors in response to electric field was visualized and recorded by the optical microscope.

3. Results and discussion

3.1 Generation of Janus droplets with different particle coverage

The Janus droplets are formed by moving the Al particles in the oil droplets initially to the oil-water interface through vibration, as shown in Figure 1(a). Under vibration, the oil phase is emulsified into small droplets, which are stabilized by the surfactant molecules in the aqueous. At the same time, the Al particles with the diameter of 10 μm moved to the oil-water interface. Generally, with the adsorption of one particle from the bulk phase to the oil-water interface, the free energy of the system decreases. The larger the reduction of the free energy, the more stable the particle at the interface. For a spherical particle with radius r at the oil-water interface, the reduction in the free energy ΔF is obtained [36,37]:

$$\Delta F = -\pi r^2 \gamma_{ow}(1 - cos\theta_w)^2 \quad \text{for } \theta_w < 90° \qquad (1)$$

$$\Delta F = -\pi r^2 \gamma_{ow}(1 + cos\theta_w)^2 \quad \text{for } \theta_w > 90° \qquad (2)$$

where, γ_{ow} is the specific interfacial free energy (i.e., interfacial tension) of the oil-water interface, θ_w is the contact angle of the particle in water. As shown in these equations, the reduction of the free energy (ΔF) increases with particle size r and oil-water interfacial free energy γ_{ow}. Therefore, by utilizing the micron sized particles, instead of nanoparticles, the adsorption of particles at the oil-water interface is energetically favorable. As demonstrated in the experimental studies of this paper, the Al particles can stay stably on the droplet surface in 2% Triton X-100 solutions with pH value ranging from 7 to 14. After Al particles adsorb to the oil-water interface, they move and accumulate to the bottom side of each droplet under gravity effect. Finally, the particles are held together to form rigid layers of solid particles on the oil droplets. Due to the capillary forces between the solid particles, the attractive interactions between particles are strong, which is difficult to disperse them again once the particle film is formed[38].

The particle coverage of the Janus droplets is dependent on the concentration of particle-in-oil dispersion. By comparing the microscope images of Janus droplets (shown in Figure 1(b)-(h)), it can be found that the particle coverage increases with the particle concentration of the dispersion. This can be understood easily. With other parameter fixed, as the particle concentration in the oil phase increases, the total number of Al particles adsorbing on the oil droplets increases; therefore, after accumulation, the particle coverage of the Janus droplets increases. As shown in Figure 1(b), at the concentration of 40 mg/mL, only limited numbers of particles shows up on the oil droplet. By increasing the particle concentration gradually, the amount of particles on the droplet surface increases, then the final particle accumulated area (indicated as the dark area in the microscope images) increases. When the concentration of the dispersion reaches to 280 mg/mL, almost half of the oil droplet is covered by particles, and a typical "half-half" Janus droplet is formed in this way. It should be noted that, in order to visualize the particle coverage of the Janus droplets clearly by using a top-down microscope, a slight pressure difference between the reservoirs of the reaction chamber was applied to drive the droplets to move very slowly with the hemisphere carrying the particle layer facing the flow field. That is why in Figure 1 the particle covered part of the droplet faces to the right side, instead to the bottom side. The relationship between the concentration of Al particle-in-oil dispersion and the particle coverage of the Janus droplet has been plotted as Figure S3. Under each condition, 20 independent measurements were conducted

to obtain the average particle coverage and the standard deviation. As can be seen from this figure, the particle coverage highly depends on the concentration of the dispersion that the particle coverage increases significantly with the concentration of the dispersion.

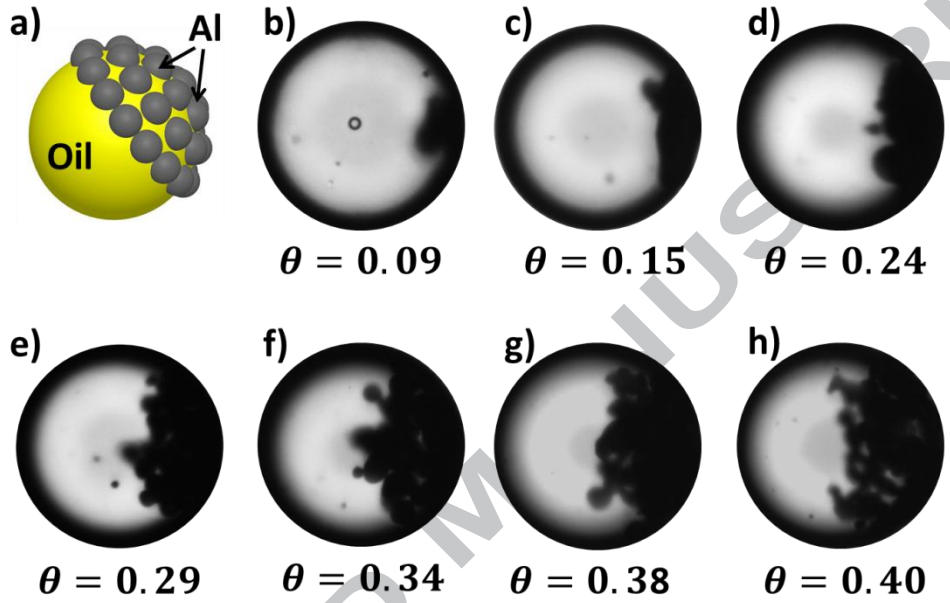

Figure 1. (a) Schematic diagram of the Janus droplet generated with Al particles. (b)-(h) Miscroscope images of Janus droplets generated with different concentrations of Al particle-in-oil dispersions: (b) 40 mg/mL, (c) 80 mg/mL, (d) 120 mg/mL, (e) 160 mg/mL, (f) 200 mg/mL, (g) 240 mg/mL and (h) 280 mg/mL. The diameter of the droplets ranges from 70 μm to 100 μm. θ is the particle coverage of the Janus droplets.

3.2 Spontaneous motion of the Janus droplets

The Janus droplet is propelled by the hydrogen bubbles that are generated by the reaction between the Al particles and the alkali solution. As illustrated in Figure 2(a), while the Janus droplet is injected into a strong alkaline medium, the protective oxide layer is removed, and the reaction between aluminum and the basic solution generates the hydrogen bubbles:

$$2Al + 2\,OH^- + 2\,H_2O \rightarrow 2\,AlO_2^- + 3\,H_2 \qquad (3)$$

Because of the hydrogen bubbles released from the particle coated side of the droplet, a driving force exerts on the droplet and pushes the droplet to move. To demonstrate the spontaneous motion of the Janus droplets in alkali solution, a Janus droplet generated from 280mg/mL particle-in-oil dispersion was injected into pH 14 NaOH solution containing 2% (v/v) Triton X-100. The non-ionic surfactant, Triton X-100, was introduced to the alkaline solution to reduce the gas-water interfacial tension, which is essential for the self-propulsion of the Janus droplet. With the effect of Triton X-100, H_2 is ejected from the surface of the Janus droplet as small bubbles. As the propelling force is linearly proportional to the total number of bubbles detached from the Janus droplet per unit time, the generation of a large number of small bubbles can generate large enough propelling force for the motion of the Janus droplet [39]. The time-lapse images of the moving droplet are shown in Figure 2(b)-(e). As shown in these figures, a trail of bubbles is ejected continuously from the Al particle side of the Janus droplet, while no bubble shows up on the oil-water interface side of the Janus droplet. This particular droplet moves at an average speed of about 25 μm/s. The speed of the Janus droplet is dependent on the balance between the bubble propelling force and the viscous drag force. Therefore, increasing of the propelling force leads to the enhancement of the speed. The trajectory of the droplet is shown in Figure 2(f). As shown in this figure, the Janus droplet moves randomly in the buffer solution, i.e., without a constant direction, due to the non-uniform bubble generation of different Al particles. This behavior is identical for essentially all self-propelling droplets. However, most trajectories of the solid Janus particles are circular or linear as reported in some published papers [40–42]. The video showing the self-propulsion motion of a Janus droplet is given in ESI as Video 1.

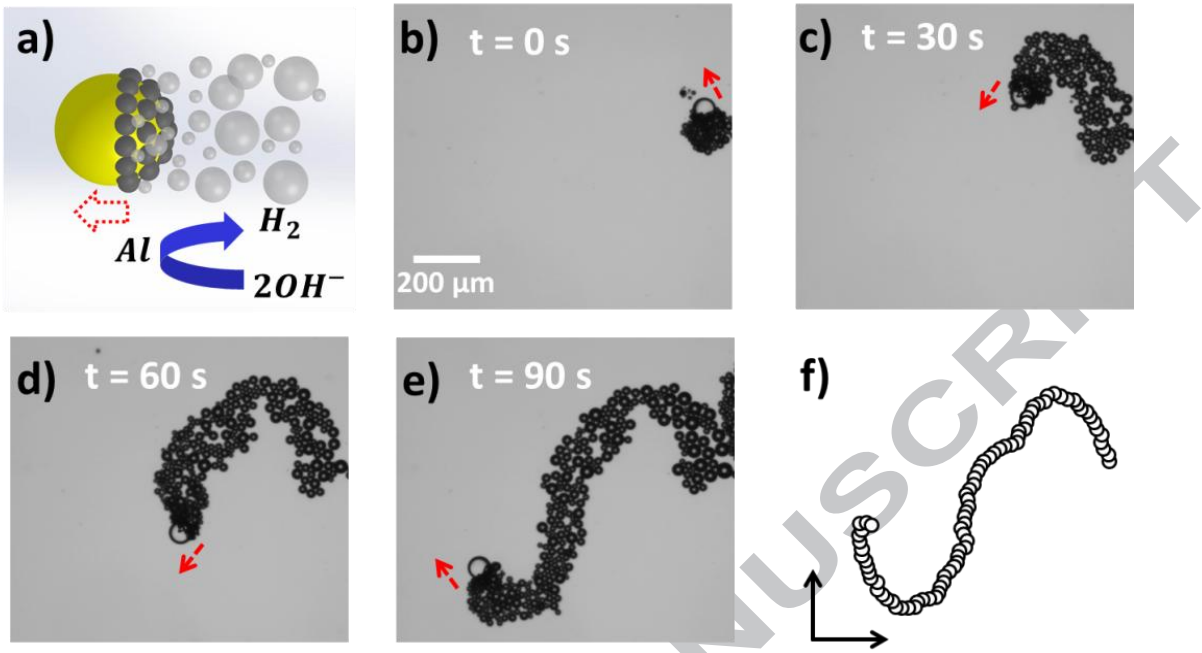

Figure 2. (a) Schematic diagram of the propulsion mechanism. (b)-(e) Time-lapse images of the spontaneous motion of a Janus droplet generated from 280 mg/mL particle-in-oil dispersion in pH 14 basic solution. (f) Trajectory of the spontaneous motion of the droplet. The diameter of the droplet is 85 µm. The concentration of Triton X-100 in the basic solution is 2% (v/v).

Speed evolution of the droplet

The speed of the Janus droplet changes with time due to the variation of the bubble generation rate. Generally, with the increase of the number of bubbles detached from the droplet, the propelling force increases; hence, the speed of the droplet increases.

For an Al particle immersed in a basic solution, the reaction between them can be divided into three periods. As the Al particle is covered with a passivation oxide layer, when the particle starts contacting with the basic solution, the strong alkaline medium reacts with the oxide layer. With the removal of this passivation oxide layer, aluminum in the core of the particle is exposed to the solution and the reaction (Eq. (3)) starts, generating hydrogen bubbles. In this period, the bubble generation rate increases quickly with time. After the entire oxide layer is removed through corrosion, the reaction moves to a stable period and the bubble generation rate reaches the highest level. In the last period, the amount of aluminum in the particle reduces due to

reaction; consequently, the bubble generation rate declines until all of the aluminum is consumed. Correspondingly, the self-propulsion of the Janus droplet undergoes three periods: initial development stage, stable stage and decline stage. The speed of the droplet increases initially, then remains constant for a while, and finally declines.

To study the speed variation with time, the Janus droplets generated from 280 mg/mL particle-in-oil dispersion were injected into basic solution at pH 14 with 2% (v/v) Triton X-100. The diameter of the Janus droplets ranges from 70 μm to 100 μm. The speed evolution of the droplets is plotted in Figure 3. As shown in this figure, during the first 10 second, the reaction between the oxide layer and the alkaline medium takes place and the Janus droplets remain still. In the next 20 second, with the removal of the oxide layer, aluminum starts to react with the alkaline solution to generate hydrogen bubbles. As the bubble generation rate increases with time, the speed of the droplets increases quickly. After the oxide layer is removed, the reaction between Al particles and basic solution reaches a stable period, and the droplets move at a constant speed of about 25 μm/s. This stable period remains approximately for 2 minutes (from 30s to 150s). After this period, the amount of bubbles generated from the droplets decreases and the speed of the droplets declines gradually. The result shown in Figure 3 is an average of 5 independent Janus droplets.

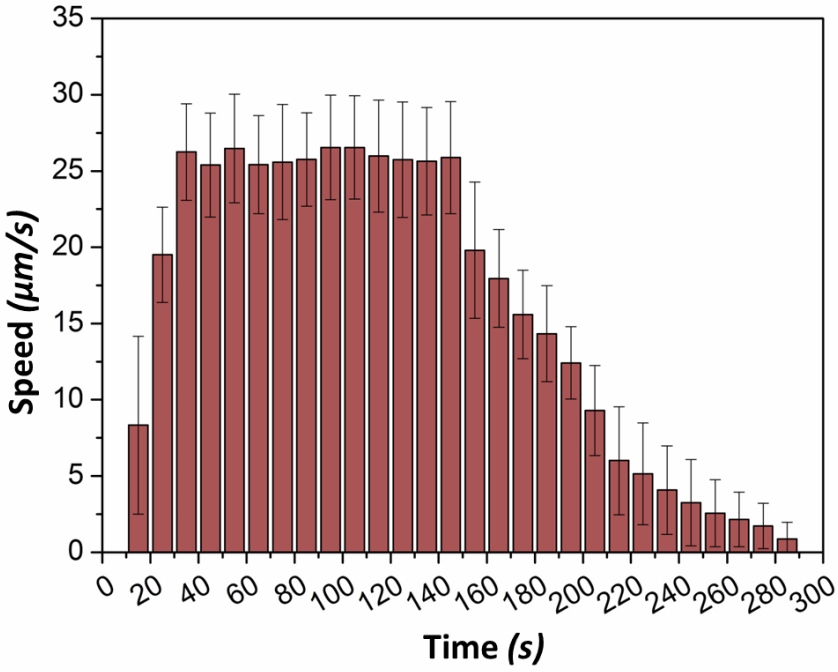

Figure 3. Speed evolution of the Janus droplets generated from 280 mg/mL particle-in-oil dispersion in pH 14 solution with 2% (v/v) Triton X-100. The diameter of the droplets ranges from 70 μm to 100 μm.

Effect of pH on speed and lifetime of the Janus droplet motion

The speed and lifetime of the Janus droplet motion are strongly dependent on the pH value of the basic solution. The hydrogen generation from the reaction between aluminum and alkali solution has been studied in many published papers [43,44]. By immersing aluminum into alkali solutions with different concentrations and measuring the volume of hydrogen, it was found that in the same amount of time, more hydrogen can be generated with higher alkali concentration. Therefore, in a higher pH solution, the bubble generation rate from the Al particle layer is larger, which leads to larger propelling force and faster spontaneous motion of the Janus droplet. However, when the reaction between aluminum and alkali solution is faster, the aluminum on the droplet surface will be consumed more quickly, and hence the lifetime of the Janus droplet motion is reduced. The variations of the speed and the lifespan of the Janus droplet motion with the pH value of the alkali solution were investigated and the results are shown in Figure 4. As

indicated in this figure, the spontaneous motion of the Janus droplets can be actuated only in strong enough alkaline medium with the critical pH value of 12.8. For the media with pH value larger than 12.8, the speed of the Janus motor has a positive relationship with the pH value while the lifetime has a negative relationship with it, which agrees with the analysis above. For pH smaller than 12.8, no bubble or only fewer bubbles are generated from the Janus droplet, and, the droplet remains stationary. It should be noted that, in this figure, in order to increase accuracy, the speeds of the droplets in the stable period were measured and analyzed.

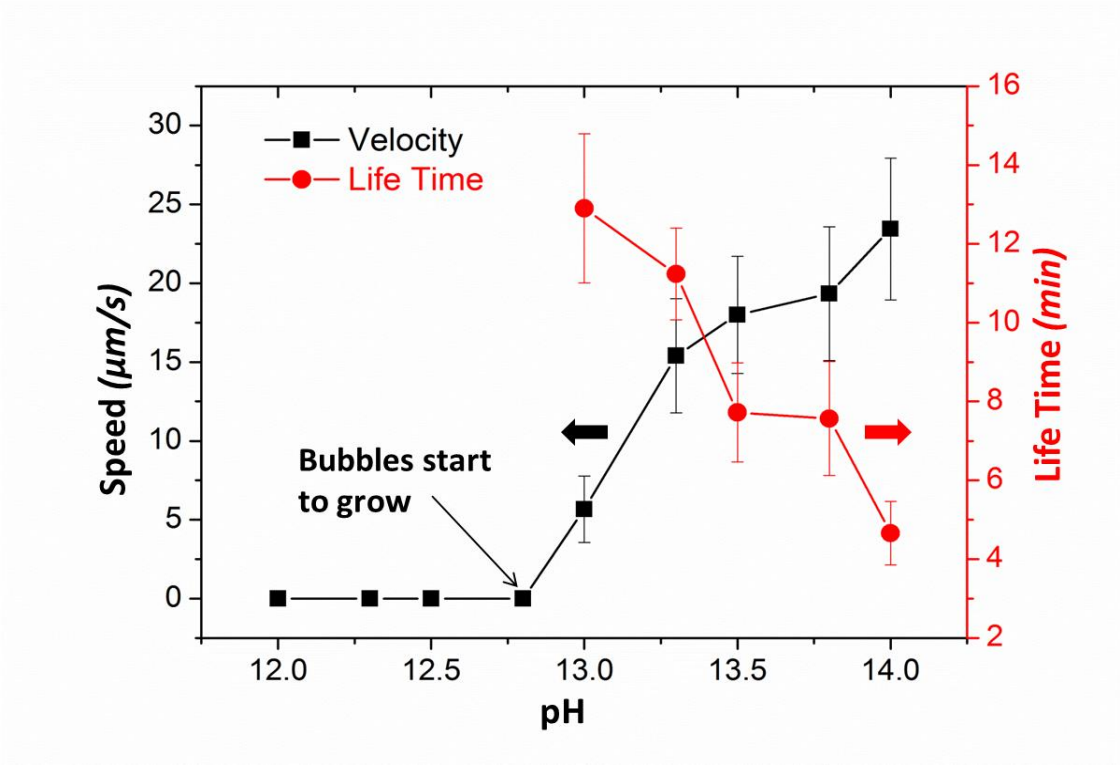

Figure 4. Dependence of the speed and lifetime of the Janus droplet motion on the pH value of the alkali solution. The Janus droplets are developed from 280 mg/mL particle-in-oil dispersion. The diameter of the Janus droplets is approximately 85 μm. The concentration of Triton X-100 in the alkali solutions is 2% (v/v).

Effect of particle coverage on speed of the Janus droplets

The particle coverage of a Janus droplet is another factor that affects the speed of it. Generally, with the increase of the particle coverage, more bubbles can be ejected from a larger Al particle

layer. With the increase of the bubble generation rate, the bubble propelling force acting on the droplet becomes larger, which drives the Janus droplet to move faster. To examine the particle coverage effect, the Janus droplet generated from different concentrations of particle-in-oil dispersions were added into pH 14 alkali solution, respectively, and the stable speeds of them were measured and plotted in Figure 5. As shown in this figure, with the increase of the concentration of dispersion, the particle coverage increases, and the speed of the droplet increases. It should be noted that only limited number of particles show up on the droplets generated from 40 mg/mL particle-in-water dispersion. Therefore, the bubble generation rate from these droplets in the basic solution is very low, and consequently, the bubble propelling force is too weak to drive the droplets to move.

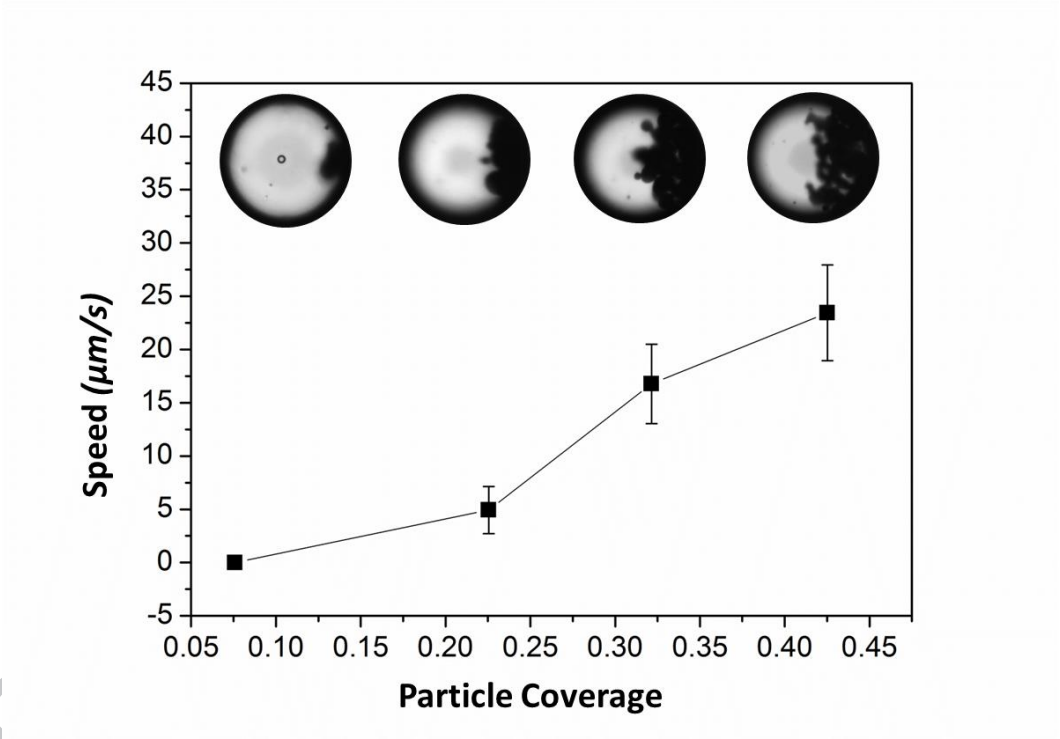

Figure 5. Dependence of the speed of the Janus droplet on the particle coverage. The Janus droplets with different particle coverages are generated from 40 mg/mL, 120 mg/mL, 200 mg/mL and 280 mg/m particle-in-oil dispersions, respectively. The surrounding alkali solution is at pH 14 and contains 2% (v/v) Triton X-100. The diameter of the Janus droplets ranges from 70 μm to 100 μm.

Effect of surfactant

Surfactant plays a very important role in the bubble-propelled motion of Janus droplets. With the presence of surfactant, the interfacial tension is reduced, and that is essential for the detachment of bubble from the droplet. As shown in Wang's work [45], the speed of the micromotor keeps increasing with the surfactant concentration before reaching the critical micelle concentration (CMC). After CMC, the velocity of the micromotor remains constant. In this paper, to control the surfactant concentration effect, Triton X-100 solution with a concentration above CMC was employed for the studies of the effects of the time evaluation, pH and particle coverage.

The spontaneous motion of the Janus droplets differs significantly in different surfactant solutions. To study the effect of the surfactant type, the performances of the droplets in different surfactant solutions of Tween 20 (nonionic), SDS (anionic) and CTAB (cationic) were tested, respectively, and the results were shown in Figure 6. As shown in Figure 6(a), in the presence of nonionic surfactant Tween 20, one large gas bubble is generated on the oil droplet. Since the bubble does not detach from the Janus droplet, the droplet does not move. This phenomenon results from the degradation of Tween 20 in alkaline solution[46–48]. Tween 20 is a polyoxyethylene sorbitol ester. In strong alkaline solutions, the hydrolysis of the ester bond takes place, which leads to the surfactant losing its functions. As shown in Figure S4(a), resulting from the ester hydrolysis, the mixture is solidified 1 hour after adding Tween 20 in a pH 14 solution. Due to the degradation of the surfactant, the interfacial tensions of oil-water interface and bubble-water interface becomes larger than that of oil-bubble interface, and the partial engulfment of the Janus droplet by the gas bubble occurs [49,50]. As shown in Figure 6(b), in SDS solution, the Janus droplet was surrounded by several larger gas bubbles and no significant translation of the Janus droplet was observed. Generally, in a strong NaOH solution, the presence of sodium ions affects the hydrolysis of SDS [51]. The SDS precipitation occurs in the solution and only limited amount of surfactant dissolves (as shown in Figure S4(b)). Therefore, the detachment of the bubbles was restrained due to relatively large interfacial tension and several large bubbles presented around the Janus droplet. As a result, no enough driving force can be generated to propel the Janus droplet to move. As shown in Figure 6(c), CTAB affects the Janus droplet by detaching Al particles from the oil-water interface. CTAB is cationic surfactant which can convert the zeta potential of the oil droplet surface from negative to positive[52]. As the

oxide layer on the Al particle also carries positive charges in aqueous solution, the electrostatic interaction between the Al particle and the interface repels the particle away from the oil-water interface[53,54]. Compared with these three surfactants listed above, Triton X-100 performs well in the spontaneous motion of Janus droplets. Different from Tween 20 and SDS, the function of Triton X-100 remains stable in NaOH solution. As shown in Figure 2, in alkaline Triton X-100 solution, numerous small gas bubbles are ejected from the Al particles adhering on the Janus droplet. With the propulsion of these gas bubbles, the spontaneous motion of the Janus droplet was generated. In conclusion, except Triton X-100, the other three surfactants, Tween 20, SDS and CTAB, are unsuitable for generating the spontaneous motion of the Janus droplets.

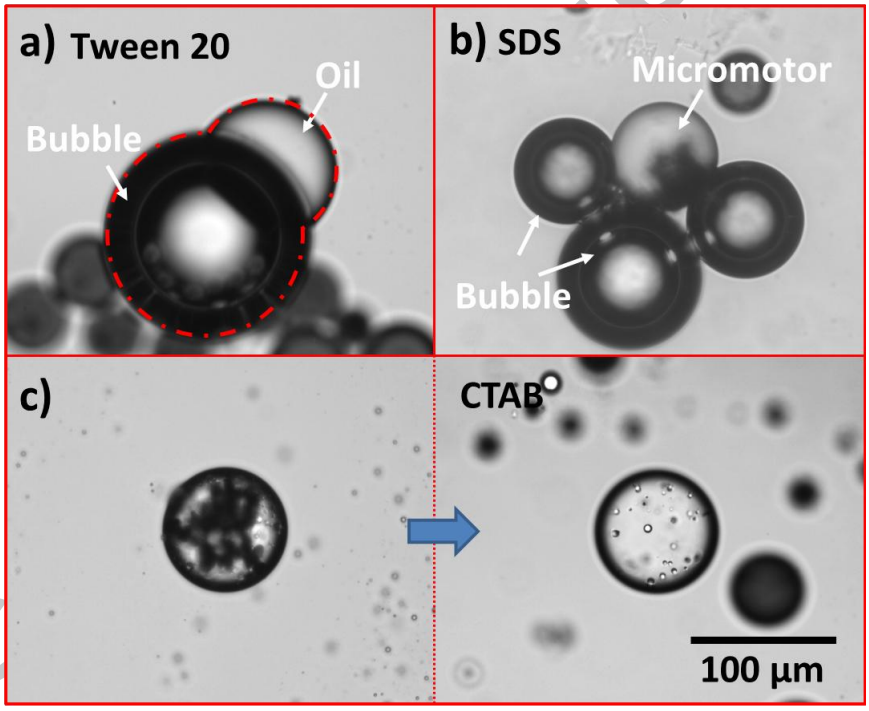

Figure 6. Effect of surfactant type on the Janus droplet. (a) A Janus droplet attached with a large gas bubble in 2% (v/v) Tween 20 solution; (b) A Janus droplet is surrounded by several large bubbles in 1.2% (w/v) SDS solution; (c) After adding 1% (w/v) CTAB solution, the particles adhering on the oil droplet surface are detached. The pH value of the surfactant solutions are 14.

3.3 Directional transport of the Janus droplets by electric field

Controllable transport of droplets is essential in many applications, including chemical analysis, biological analysis and cargo delivery. For example, the droplet can be used as a micro-reactor for biochemical reaction and a carrier transporting organic substances and biomolecules. Furthermore, combining the motion of Janus droplets with the microfluidic technology offers the chance to develop novel droplet-based microfluidics systems for synthesis, analysis and detection without the need of external propulsion.

In this work, in order to direct the spontaneous motion of the Janus droplets, an external DC electric field was applied. As the Janus droplet has a higher density on the particle coated side than that of the other side ($\rho_{al} > \rho_{oil}$), the accelerations of the two sides are different under the hydrodynamic force, and the lighter side moves faster than the heavier side. As a result, the Janus droplet rotates with the oil side forwarding the direction of the hydrodynamic force. Under externally applied electric field, electroosmotic flows are generated on the surfaces of the reaction chamber and the Janus droplet. With the effect of the electroosmotic flows, a hydrodynamic force is exerted on the Janus droplet, which forwards the Janus droplet to get aligned with the electric field. It should be noted that as the self-propulsion motion of the Janus droplet takes place in a strong alkaline solution, applying an electric field to the system continuously will cause electrolysis and Joule heating. To avoid these effects in the experiment, weak electric field of 25V/cm with a time interval of 2s was applied intermittently to control and adjust the moving direction. Figure 7(b)-(d) show the change of the moving direction of the Janus droplet under the applied electric field. It can be seen that by applying electric field intermittently, the Janus droplet rotates, changes its direction, and finally get aligned with the direction of the electric field.

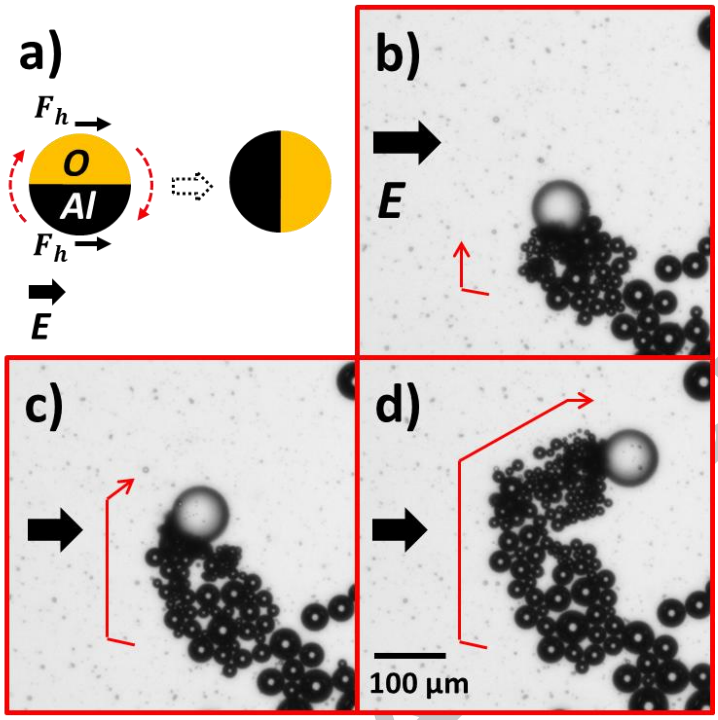

Figure 7. (a) Schematic of the rotation of the Janus droplet under electric field; (b)-(d) Time-lapse images of the direction change of the moving Janus droplet generated from 200 mg/mL particle-in-oil dispersion under intermittent applying electric field of 25 V/cm. The red lines in (b)-(d) indicate the trajectories.

The directionally controlled transportation of the Janus droplet was demonstrated by making the droplet to move linearly and to make a sharp turn. As shown in Figure 8(a), the Janus droplet moves linearly from left to right in response to the electric field. The motion of the droplet was monitored under a microscope, and the electric field was applied intermittently only when the Janus micromotor went out of the designed track. Therefore, the effect of electroosmotic flow on the motion of the droplet is limited. The turning of the Janus droplet was achieved by changing the direction of electric field. As shown in Figure 8(b) and (c), initially, the intermittent electric field (E1) was applied transversely (from left to right), and the Janus droplet moves from left to right responsively. Then, the direction of the applied electric field was rotated 90° counterclockwise (E2). In response to the electric field of E2, the rotation of the Janus droplet took place and the Janus droplet moved vertically to its original direction. The video showing the electric-control-turning of the self-propelled Janus droplet is available in ESI as Video 2.

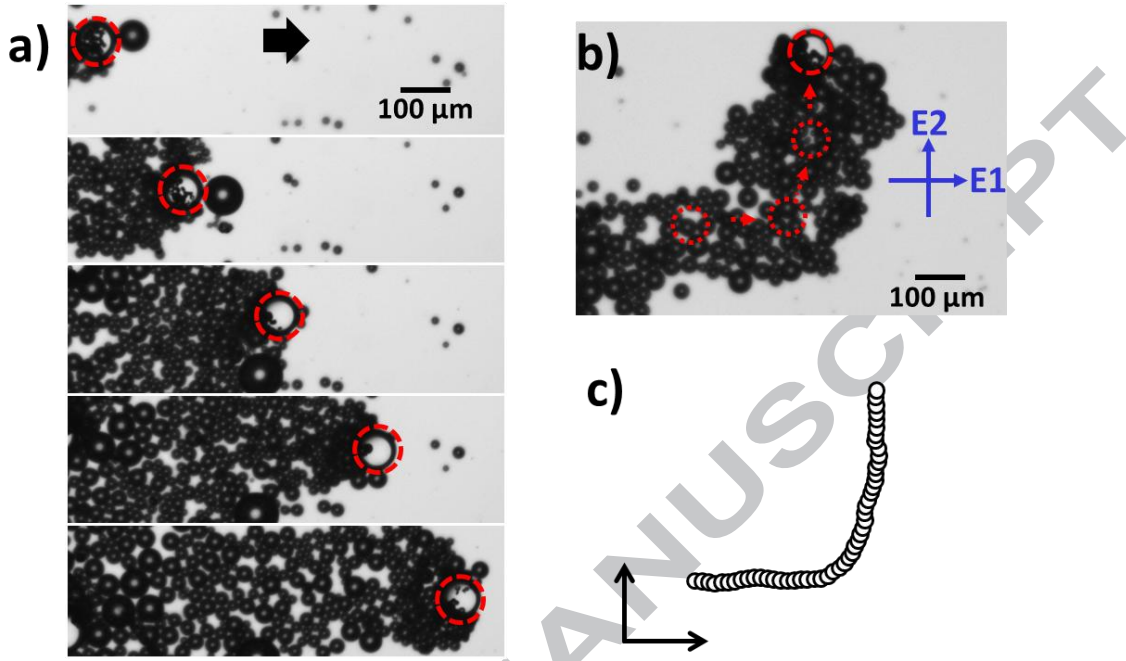

Figure 8. (a) Time-lapse images of the linear motion of a Janus droplet under the control of electric field. (b) 90° turning of the droplet with the direction change of the electric field. The blue arrows indicate the directions of the electric fields (c) Trajectory of the droplet turning 90° by changing the direction of the electric field 90° counterclockwise. In the experiments, the Janus droplets were developed from 200 mg/mL particle-in-oil dispersion and the strength of the control electric field is 25 V/cm.

4. Conclusion

Self-propelled motion of Janus droplets powered by the reaction of aluminum particles with alkaline solution was studied in this paper. The Janus droplets are fabricated by covering one side of oil droplets with aluminum particles. The Janus droplets with different particle coverages were generated by using different concentrations of particle-in-oil dispersions. The particle coverage of the Janus droplets increases with the particle dispersion concentration. The spontaneous motion of the Janus droplets in NaOH solution was demonstrated. The gas bubbles are generated through the chemical reaction from the particle-coated side, the detaching of the

gas bubble from the Janus droplet pushes the droplet to move towards the side without the presence of particles. The effects of time, pH of the alkaline solution, particle coverage and surfactant in the solution on the speed of the Janus droplet were tested experimentally. Generally, over the course of time, the Janus droplet experiences three periods that the speed of the Janus droplet increases initially, then remains constant, and finally declines. The average moving speed of the Janus droplets increases with pH of the alkaline solution and the particle coverage of the droplet. In comparison with Tween 20, SDS and CTAB, surfactant Triton X-100 is most suitable for the generation of spontaneous motion of Janus droplets. The controlled directional motion of the Janus droplets by using electric field was also demonstrated successfully.

Acknowledgements

The authors wish to thank the financial support of the Natural Sciences and Engineering Research Council (NSERC) of Canada through a research grant (RGPIN-03622) to D. Li.

References

[1] R. Seemann, M. Brinkmann, T. Pfohl, S. Herminghaus, Reports Prog. Phys. 75 (2012) 16601.

[2] L. Mazutis, J. Gilbert, W.L. Ung, D.A. Weitz, A.D. Griffiths, J.A. Heyman, Nat. Protoc. 8 (2013) 870–891.

[3] Y. Zhu, Q. Fang, Anal. Chim. Acta 787 (2013) 24–35.

[4] S.Y. Teh, R. Lin, L.H. Hung, A.P. Lee, Lab Chip 8 (2008) 198.

[5] Z. Wang, J. Zhe, Lab Chip 11 (2011) 1280.

[6] T.P. Lagus, J.F. Edd, J. Phys. D. Appl. Phys. 46 (2013) 114005.

[7] T. Toyota, N. Maru, M.M. Hanczyc, T. Ikegami, T. Sugawara, J. Am. Chem. Soc. 131 (2009) 5012–5013.

[8] T. Ban, K. Tani, H. Nakata, Y. Okano, Soft Matter 10 (2014) 6316–6320.

[9] K. Nagai, Y. Sumino, H. Kitahata, K. Yoshikawa, Phys. Rev. E 71 (2005) 65301.

[10] V. Pimienta, M. Brost, N. Kovalchuk, S. Bresch, O. Steinbock, Angew. Chemie - Int. Ed. 50 (2011) 10728–10731.

[11] D. Molin, R. Mauri, V. Tricoli, Langmuir 23 (2007) 7459–7461.

[12] T. Ban, T. Yamada, A. Aoyama, Y. Takagi, Y. Okano, Soft Matter 8 (2012) 3908.

[13] J.M.P. Gutierrez, T. Hinkley, J.W. Taylor, K. Yanev, L. Cronin, Nat. Commun. 5 (2014) 5571.

[14] A.M. Cazabat, F. Heslot, S.M. Troian, P. Carles, Nature 346 (1990) 824–826.

[15] A. Diguet, R.M. Guillermic, N. Magome, A. Saint-Jalmes, Y. Chen, K. Yoshikawa, D. Baigl, Angew. Chemie - Int. Ed. 48 (2009) 9281–9284.

[16] K. Ichimura, S.K. Oh, M. Nakagawa, Science 288 (2000) 1624–1626.

[17] L. Florea, K. Wagner, P. Wagner, G.G. Wallace, F. Benito-Lopez, D.L. Officer, D. Diamond, Adv. Mater. 26 (2014) 7339–7345.

[18] Y.Y. Lin, E.R.F. Welch, R.B. Fair, Sensors Actuators, B 173 (2012) 338–345.

[19] C.G. Cooney, C.Y. Chen, M.R. Emerling, A. Nadim, J.D. Sterling, Microfluid. Nanofluid. 2 (2006) 435–446.

[20] J. Čejková, M. Novák, F. Štěpánek, M.M. Hanczyc, Langmuir 30 (2014) 11937–11944.

[21] T. Ban, H. Nakata, J. Phys. Chem. B 119 (2015) 7100–7105.

[22] B. Jurado-Sánchez, M. Pacheco, R. Maria-Hormigos, A. Escarpa, Appl. Mater. Today 9 (2017) 407–418.

[23] L. Liu, T. Bai, Q. Chi, Z. Wang, S. Xu, Q. Liu, Q. Wang, Micromachines 8 (2017) 267.

[24] Z. Wu, X. Lin, T. Si, Q. He, Small 12 (2016) 3080–3093.

[25] R. Dong, Y. Hu, Y. Wu, W. Gao, B. Ren, Q. Wang, Y. Cai, J. Am. Chem. Soc. 139 (2017) 1722–1725.

[26] R. Dong, Q. Zhang, W. Gao, A. Pei, B. Ren, ACS Nano 10 (2016) 839–844.

[27] F. Mou, C. Chen, Q. Zhong, Y. Yin, H. Ma, J. Guan, ACS Appl. Mater. Interfaces 6 (2014) 9897–9903.

[28] S. Simoncelli, J. Summer, S. Nedev, P. Kühler, J. Feldmann, Small 12 (2016) 2854–2858.

[29] W. Gao, M. D'Agostino, V. Garcia-Gradilla, J. Orozco, J. Wang, Small 9 (2013) 467–471.

[30] M. Li, D. Li, Electrophoresis 38 (2017) 287–295.

[31] M. Li, D. Li, J. Chromatogr. A 1501 (2017) 151–160.

[32] M. Li, D. Li, Microfluid. Nanofluid. 21 (2017) 16.

[33] M. Li, D. Li, Microfluid. Nanofluid. 20 (2016) 79.

[34] M. Li, D. Li, J. Nanopart. Res. 18 (2016) 120.

[35] M. Li, D. Li, Adv. Colloid Interface Sci. 236 (2016) 142–151.

[36] R. Aveyard, B.P. Binks, J.H. Clint, Adv. Colloid Interface Sci. 100–102 (2003) 503–546.

[37] B.P. Binks, Curr. Opin. Colloid Interface Sci. 7 (2002) 21–41.

[38] B. Wang, M. Wang, H. Zhang, N.S. Sobal, W. Tong, C. Gao, Y. Wang, M. Giersig, D. Wang, H. Möhwald, Phys. Chem. Chem. Phys. 9 (2007) 6313.

[39] J.G. Gibbs, Y.P. Zhao, Appl. Phys. Lett. 94 (2009) 163104.

[40] K.P. Yuet, D.K. Hwang, R. Haghgooie, P.S. Doyle, Langmuir 26 (2010) 4281–4287.

[41] W. Gao, A. Pei, J. Wang, ACS Nano 6 (2012) 8432–8438.

[42] A.X. Lu, Y. Liu, H. Oh, A. Gargava, E. Kendall, Z. Nie, D.L. Devoe, S.R. Raghavan, ACS Appl. Mater. Interfaces 8 (2016) 15676–15683.

[43] C.B. Porciúncula, N.R. Marcilio, I.C. Tessaro, M. Gerchmann, Brazilian J. Chem. Eng. 29 (2012) 337–348.

[44] C.C. Wang, Y.C. Chou, C.Y. Yen, Procedia Eng. 36 (2012) 105–113.

[45] H. Wang, G. Zhao, M. Pumera, J. Phys. Chem. C 118 (2014) 5268–5274.

[46] K. Nidhi, S. Indrajeet, M. Khushboo, K. Gauri, D.J. Sen, Int. J. Drug Dev. Res. 3 (2011) 26–33.

[47] Y. Li, D. Hewitt, Y.K. Lentz, J.A. Ji, T.Y. Zhang, K. Zhang, Anal. Chem. 86 (2014) 5150–5157.

[48] A.C. McShan, P. Kei, J.A. Ji, D.C. Kim, Y.J. Wang, PDA J. Pharm. Sci. Technol. 70 (2016) 332–345.

[49] J. Guzowski, P.M. Korczyk, S. Jakiela, P. Garstecki, Soft Matter 8 (2012) 7269–7278.

[50] L. Ge, S.E. Friberg, R. Guo, Curr. Opin. Colloid Interface Sci. 25 (2016) 58–66.

[51] A.L. Gray, J.T. Hsu, J. Chromatogr. A 824 (1998) 119–124.

[52] Y. Gu, D. Li, J. Colloid Interface Sci. 206 (1998) 346–349.

[53] M.M. Ramos-Tejada, J.D.G. Dura, A. Ontiveros-Ortega, M. Espinosa-Jimenez, R. Perea-Carpio, E. Chibowski, Colloids and Surfaces 24 (2002) 309–320.

[54] V.S. Nguyen, D. Rouxel, R. Hadji, B. Vincent, Y. Fort, Ultrason. Sonochem. 18 (2011) 382–388.

Graphical abstract